NUTRIENT DYNAMICS ALONG A NEW YORK BIGHT TRANSECT AT LONG BRANCH, NEW JERSEY FROM MAY TO OCTOBER 1983

by

Ruth Waldhauer, A. F. J. Draxler, A. Matte,
P. Lyons, D. McMillan and G. Pyramides

U. S. Department of Commerce
NOAA, NMFS
Northeast Fisheries Center
Sandy Hook Laboratory
Highlands, New Jersey 07732

Sandy Hook Report No. SHL 84-12

Waters of the sewage polluted New York Bight apex have the highest rate of phytoplankton primary productivity (2.3 g $C/m^2/d$) of the continental shelf between Cape Hatteras and Canada (O'Reilly and Bush, 1984). The inshore coastal zone south of the New York Bight apex is also very productive (1.38 g $C/m^2/d$) surpassing even the well-mixed central area of the Georges Bank (1.25 g $C/m^2/d$) (O'Reilly, Zetlin, Busch, in prep). This coastal zone area also experiences periodic dissolved oxygen depletion due to high BOD loading although the ultimate source of this loading (autochtonous vs allochthonous) is not clear (Thomas et al., 1979). In general primary production rates are at least partially determined by the availability of nutrients. In the coastal zone nutrients are provided to the phytoplankton from four sources: 1) land-derived sources by way of estuarine outflows; 2) onshore intrusions of nutrient-rich deeper water followed by vertical mixing; 3) in situ remineralization of organic matter; and 4) water mass advection. For example, in the New York Bight apex, 50-70% of the nitrogen necessary to support the phytoplankton productivity in summer and 100% during the remainder of the year is supplied by outflows of the Hudson-Raritan estuary (Garside et al., 1976). A previous NEMP study based on over 50 remotely sensed images of surface turbidity, shows the location of the estuarine plume usually in a position near the New Jersey coast (Fedosh and Munday 1982) suggesting a direct contribution to the nutrient budget of the New Jersey inshore area.

Our study addresses the question of the relative contribution of the estuarine outflow and onwelled nutrients to phytoplankton production of the near shore coastal zone outside the apex. To study the time course of these inputs and their relationship to primary productivity, dissolved oxygen depletion rates, and marine life in general, weekly measurements of hydrographic, chemical and biological variables, along a transect off Long Branch, New Jersey (Figure 1), together with daily monitoring at the Long Branch Fishing Pier, were undertaken beginning in May 1983. These frequent weekly samplings compliment larger scaled New York Bight wide surveys which are made approximately four times during the stratified season (Whitledge et al., this annual report).

Surface Layer Nutrient Depletion

In May when sampling began the vertically uniform, high nutrient concentrations resulting from winter mixing had been reduced by the spring phytoplankton bloom (e.g. nitrate <0.8 µM). With the onset of stratification, the surface layer was depleted further. In the case of nitrate levels fell below the detection limit of our anaytical method (0.02 µM). The process of depletion was initiated offshore at station 7, where nitrate was undetectable by 10 May. It spread shoreward through June and July, interrupted by the periodic arrival of fresh, nutrient-rich estuarine water (see below) and was complete by 25 July (Figure 11).* Shallowness and relatively enhanced vertical exchange was probably responsible for the nitrate concentrations at the surface of station 2 in July and again in August. The surface layer at stations 3 to 7 remained depleted of nitrate through mid-September (Figure 18) except for major wind-induced events (e.g. 15 August; Figure 14). Unlike the

*Figures 5 through 19 are in chronological order.

pattern of depletion, resupply of nitrate with fall turnover began inshore and progressed seaward (Figure 19).

Phosphate and silicate depletions were similar to nitrogen but the time scale was somewhat different. Phosphate was depleted for the first time during the season on 24 May in surface waters at stations 6 and 7; silicate depletion on 18 July in surface waters at stations 5, 6 and 7.

Estuarine Nutrient Input to the Transect

Two major freshets associated with outflows of the Hudson and Raritan rivers (see Draxler et al., this report) brought large supplies of nutrients to the study area. The fresh water of the Raritan outflow arrived at the transect in early May with an observed maximum nitrate concentration of 9 μM at the surface of station 3, and surface salinity increased with distance from shore. The peak fresh water input at the Long Branch Pier station, 23 Km from the estuary mouth, occurred on 6 May with 21.2 μM nitrate, 47.1 μM silicate and salinity of 16.95 ppt (Figures 20, 21) suggesting that in the area of the transect the peak input arrived between 4 and 10 May samplings. This first freshening dispersed in less than a week. By the 17 May sampling, the water column was again destratified and nitrate concentration had fallen nearly tenfold measuring 2.4 μM at the surface of station 3 (Figure 5). The second freshet, observed along the transect on 1 June (Figure 6), probably resulted from Hudson River outflow. The maximum nitrate concentrations (12.6 μM) and minimum salinity (22.65 ppt) were found at station 4. This plume, centered further offshore than the previous one, affected the water column to 5 m and initiated the persistent seasonal stratification of the water column. The resulting nitrate and silicate enrichment were accompanied by a high phytoplankton biomass until July (e.g. 25 mg/m^3 at the surface at station 5 on July 6; Figure 3).

Onwelling

Onwelling of offshore bottom water was first observed on 18 July as a drop in temperature of the bottom waters at stations 6 and 7 (Figure 4) and an increase in nitrate, ammonium and phosphate concentrations (Figure 10). This onwelling extended shoreward to station 4 by 1 August. From the presence of high ammonium concentrations (e.g. 12.8 μM; Figure 11), we infer that this was "cold pool" water. The decline in dissolved oxygen in the bottom water was relieved periodically during this time and paralleled a shoreward movement of higher salinity water in the lower water column (Figures 10-12). When this process of dissolved oxygen replenishment stopped, oxygen concentration declined rapidly (see Draxler et al., this report).

Downwelling

Onwelling was interrupted by a major downwelling event culminating about 15 August. Along the transect from stations 3 to 7, nitrate and ammonium concentrations in the bottom water decreased considerably between 1 and 8 August and still further by 15 August (Figures 2, 12, 13, 14). For example, at station 4 nitrate concentrations decreased from 1.86 to 0.64 to 0.06 μM during this period.

The downward and offshore water movements were accompanied by the advection of low salinity, nutrient-rich water into the surface area of inshore stations. On 8 August (Figures 2, 13) the freshening observed at the middle of the transect contained up to 1.25 µM nitrate but little ammonium (1.5 µM). Nitrate (>1.0 µM) was found at 5 m while the surface was depleted. The nutrient distributions coincided inversely with areas of high phytoplankton biomass, 23.2 mg chla/m^3 (Figure 3), which was probably responsible for nitrate depletion at the surface. During the most intense downwelling (15 August) water at the surface of the shallow inshore stations 2, 3 and 4 were enriched. Concentrations of nitrate were 2.4, 2.8 and 1.5 µM, and of ammonium were 13.6, 10.5 and 6.6 µM, respectively, but the area of high phytoplankton biomass was centered at the offshore edge (station 4) of the nutrient-rich water (Figures 3, 14). Between 11 and 20 August there was a parallel increase in the nutrient supply at the Long Branch pier station, followed shortly by a corresponding increase in chlorophyll a (Figures 20, 21, 22).

The downwelling also forced surface waters having higher dissolved oxygen concentrations into the lower water column resulting in major reoxygenation of bottom water from stations 2 to 6.

During the following two weeks (15, 22 August) temperature and salinity stratification was reestablished (Figures 4, 15, 16) partly as a result of the shoreward movement of higher salinity water. This movement along the bottom carried moderate amounts of nitrate (1.5 µM) back into the hypopycnion with ammonium concentrations reaching 13.6 µM.

Ammonium Accumulation

On 4 May ammonium concentrations in the lower water column ranged from 1.4 to 2.3 µM except at the bottom of the deeper offshore station 7 where 9.2 µM was measured. Through the summer concentrations then increased as ammonium accumulated below the pycnocline as the result of the competing processes of organic material remineralization, diffusion, advection and, in some places, phytoplankton uptake. On a number of cruises we found that the ammonium maxima were above the bottom. This was first observed on 6 June at station 4 when the 7, 13 and 20 m samples contained 0.8, 2.9 and 1.9 µM, respectively. On 11 July a mid-water ammonium maximum extended from station 5 to 7 (10 km). In it, concentrations were >5 µM which was 2.5 to 10 times those in the samples above and below (Figure 9). With the 1% light level 2 to 7 m below the ammonium maxima and with nitrate concentrations in the range of 1 µM (precluding non-assimilative nitrate reduction) high rates of heterotrophic activity evidently were occurring in the mid-water column. Light levels were suboptimal but high enough to sustain significant rates of photosynthesis using the available ammonium. Along the transect, the lowest dissolved oxygen concentration were frequently not found near the seabed but near the bottom of the pycnocline (see Draxler, this report). This inverse relation between ammonium and dissolved oxygen is an example of the importance here of heterotrophy in the oxygen depletion process. We do not have ammonium data for the following week (18 July) but the phytoplankton biomass distribution had a mid-water maximum (where it was at the bottom of the water column on 11 July) and nitrate levels near the sediment were lower in spite of the beginning of onwelling.

Frequency of Sampling

Had sampling been less frequent than weekly in the transect area, events such as input from a spring freshet or the downwelling observed on 15 August could have been missed. While weekly sampling was fine-scaled enough to detect the presence of these events, determinations of their time of arrival and peak magnitude would require still more frequent sampling. For example, nitrate values measured at station 3 during weekly transect sampling were 0.5 μM on 4 May and 9.4 μM on 10 May while data collected daily at the Long Branch Pier station showed a maximum of 21.2 μM occurred on 6 May.

The day-to-day variability in the Long Branch Pier station data set is large. Information from the NOS tide station located on the pier can be used to quantify the variability due to tidal cycle. Frequent measurements over several diurnal cycles would allow this component of variability to be better understood.

Summary

The seasonal succession of nutrient events which control phytoplankton productivity in the study area are summarized in Figure 2. Early spring depletion of nutrients throughout the water column supports moderate phytoplankton biomass densities, about 7 mg chla/m^3 (Figure 3). Large scale nutrient enrichment occurs with periodic arrival of estuarine peak outflows in May and June. These events are accompanied by increases in biomass (to 25 mg chla/m^3) and initiate haline water column stratification. With stratification, the hyperpycnion is depleted of nitrate, and phytoplankton primary production becomes dependent on recycled nitrogen, primarily ammonium. Below the pycnocline, ammonium accumulates even within the euphotic zone and onwelling of bottom water further increases the above-below pycnocline differences. Subpycnocline phytoplankton maxima appear to be supported by these two nutrient sources at a suboptimal but sufficient light level. In 1983, a major wind-induced downwelling interrupted onwelling in mid-August. During the following weeks low nitrogen concentrations throughout the water column at mid-transect stations were associated with low phytoplankton biomass concentrations. Thereafter, onwelling resumed reintroducing nitrogen to the bottom water and stimulating primary production there. Nitrate concentrations increased until turnover in September-October when higher concentrations of phytoplankton were again in the upper water column leading to fall bloom.

REFERENCES

FEDOSH, M. S. and J. C. MUNDAY.
1982. Satellite analysis of estuarine plume behavior. NEMP Annual Report. 1982.

GARSIDE, C., P. C. MALONE, O. A. ROELS and B. A. SCHARFSTEIN.
1976. An evaluation of sewage-derived nutrients and their influence on the Hudson estuary and the New York Bight. Est. Coast. Mar. Sci. 4: 281-9.

O'REILLY, J. E. and D. A. BUSCH.
1984. Phytoplankton primary production on the northwestern Atlantic shelf. Rapp. P. V. Reun. Cons. Int. Explor. Mer, 183: 255-268.

O'REILLY, J. E., C. EVANS-ZETLIN and D. A. BUSCH.
In prep. Primary Production. In Georges Bank, R. Backus and D. Bourne (eds.). MIT Press.

THOMAS, J. P., J. E. O'REILLY, A. F. J. DRAXLER, J. A. BABINCHAK, C. N. ROBERTSON, W. C. PHOEL, R. I. WALDHAUER, C. A. EVANS, A. MATTE, M. S. COHN, N. F. NITKOWSKI and S. DUDLEY.
1979. Biological processes: Productivity and respiration. pp. 231-261. In Swanson, R. L. and C. J. Sindermann (eds.). Oxygen depletion and associated benthic mortalities in New York Bight, 1976. United States Government Printing Office, Washington, DC.

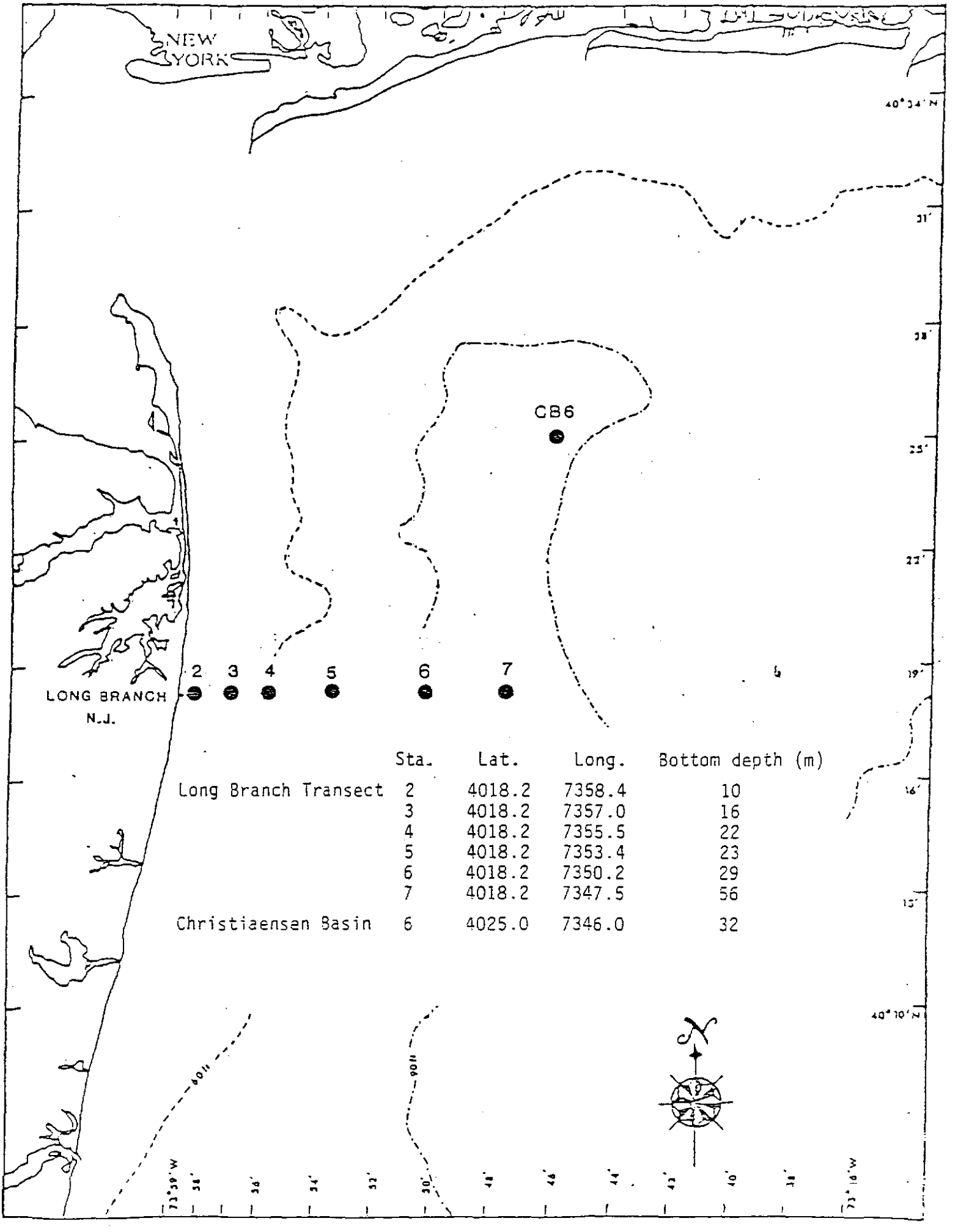

	Sta.	Lat.	Long.	Bottom depth (m)
Long Branch Transect	2	4018.2	7358.4	10
	3	4018.2	7357.0	16
	4	4018.2	7355.5	22
	5	4018.2	7353.4	23
	6	4018.2	7350.2	29
	7	4018.2	7347.5	56
Christiaensen Basin	6	4025.0	7346.0	32

FIGURE 1

NITRATE CONCENTRATIONS (uM)

from May to October 1983 (Julian Day 121 to 274)

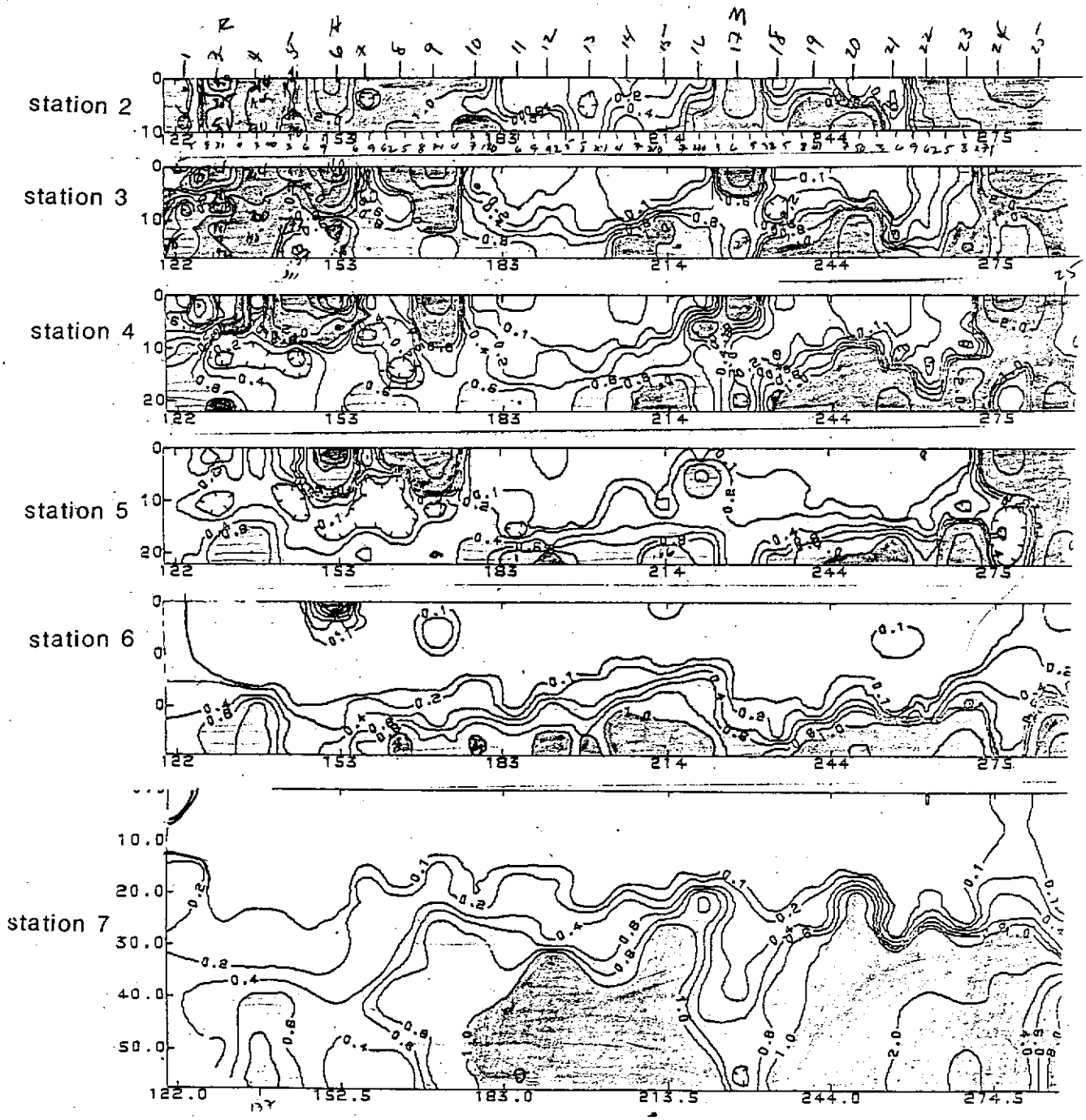

FIGURE 2

TOTAL CHLOROPHYLL-a (mg/M3)

from May to October 1983 (Julian Day 121 to 274)

(1% light depth denoted by heavy line)

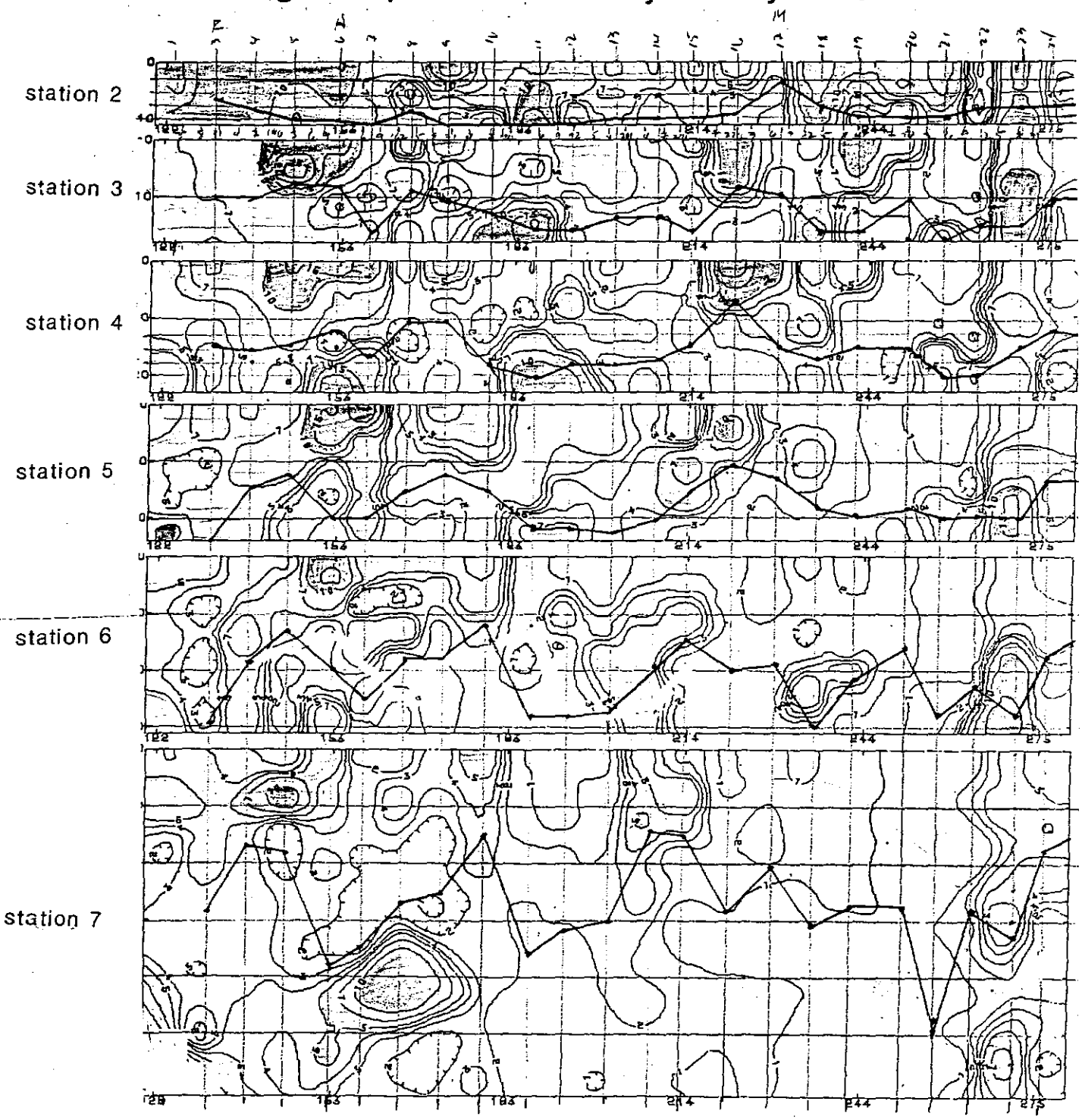

FIGURE 3

TEMPERATURE (°C)

from May to November 1983 (Julian Day 121 to 305)

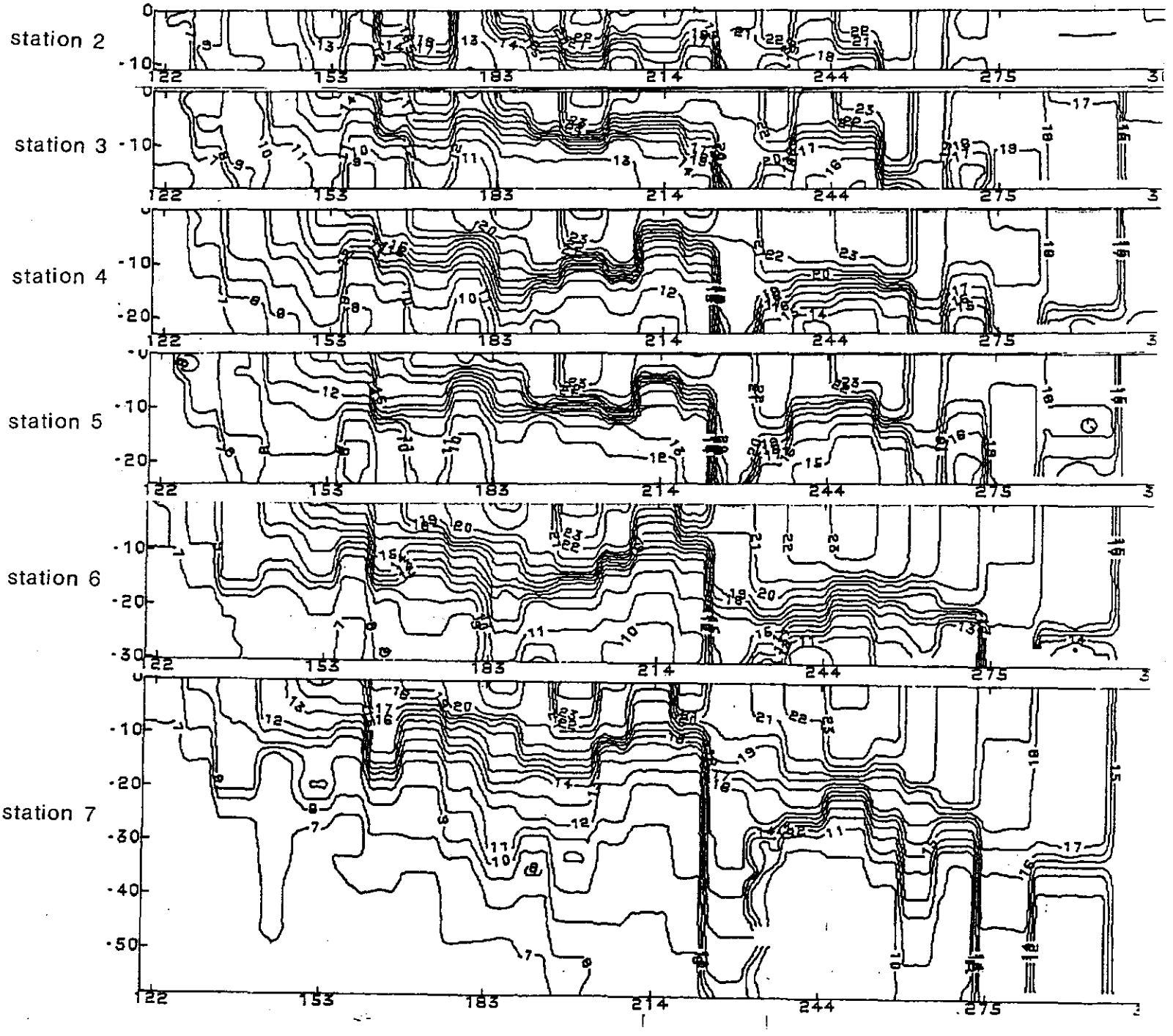

FIGURE 4

TRANSECT MONITORING

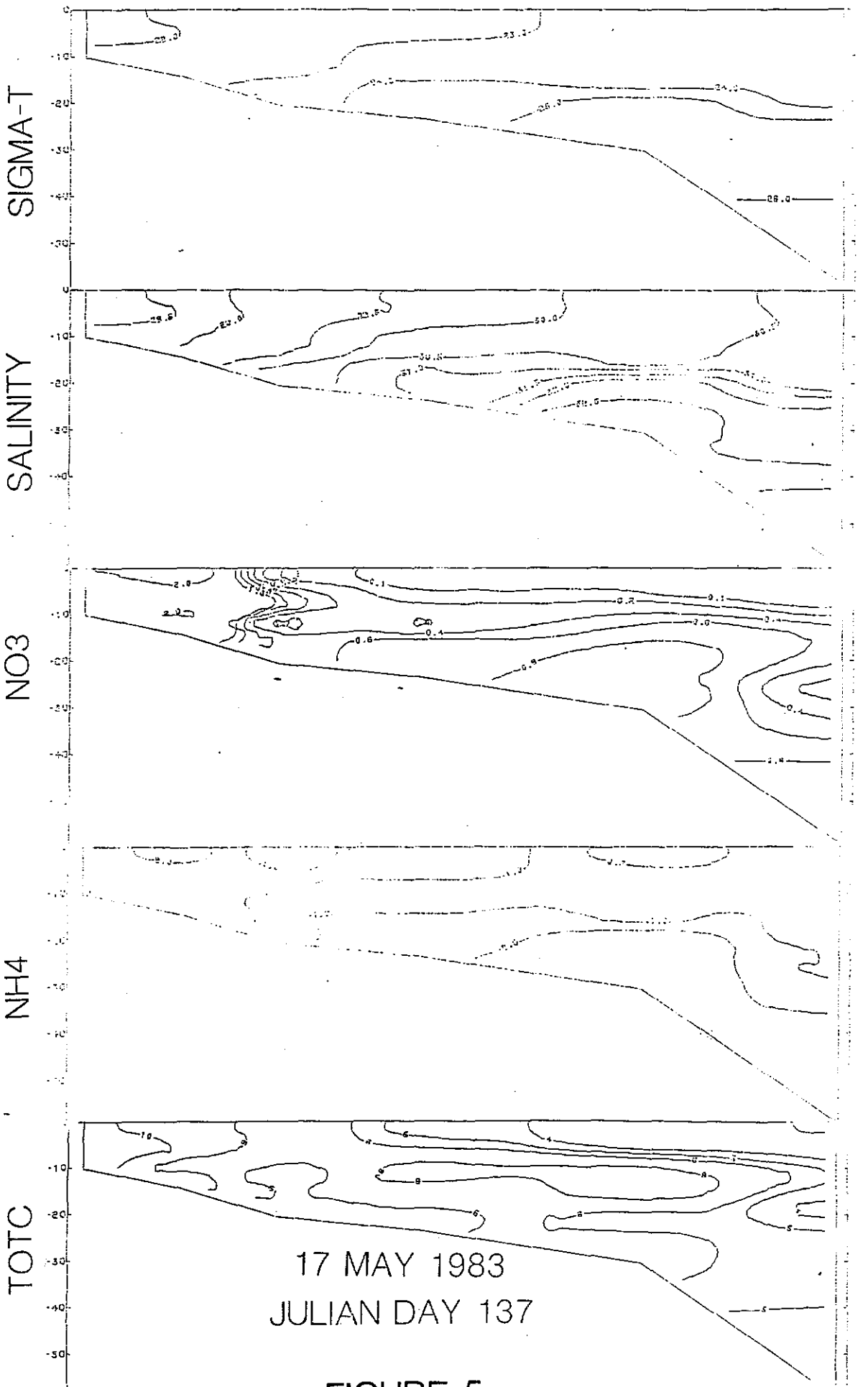

17 MAY 1983

JULIAN DAY 137

FIGURE 5

TRANSECT MONITORING

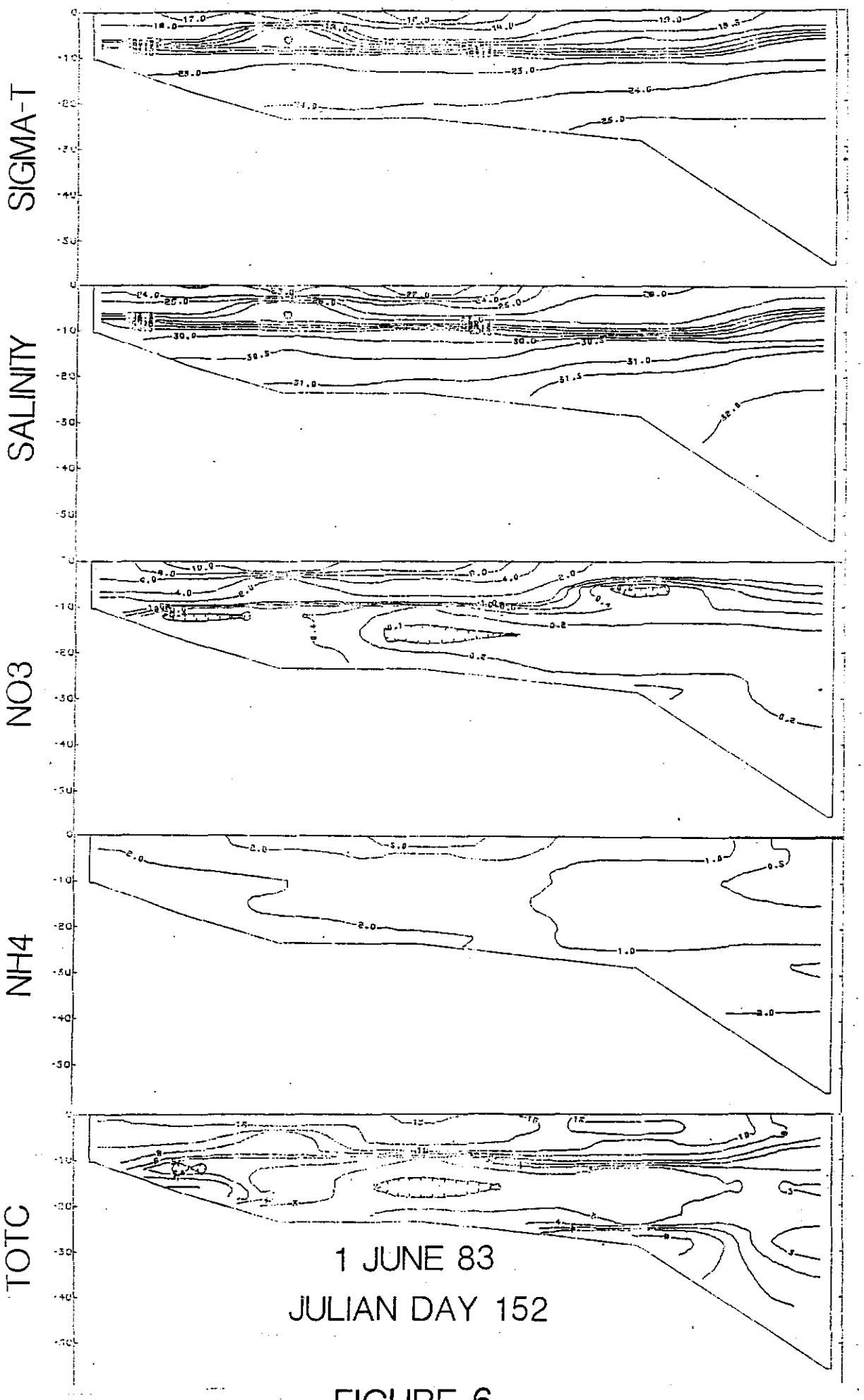

1 JUNE 83

JULIAN DAY 152

FIGURE 6

TRANSECT MONITORING

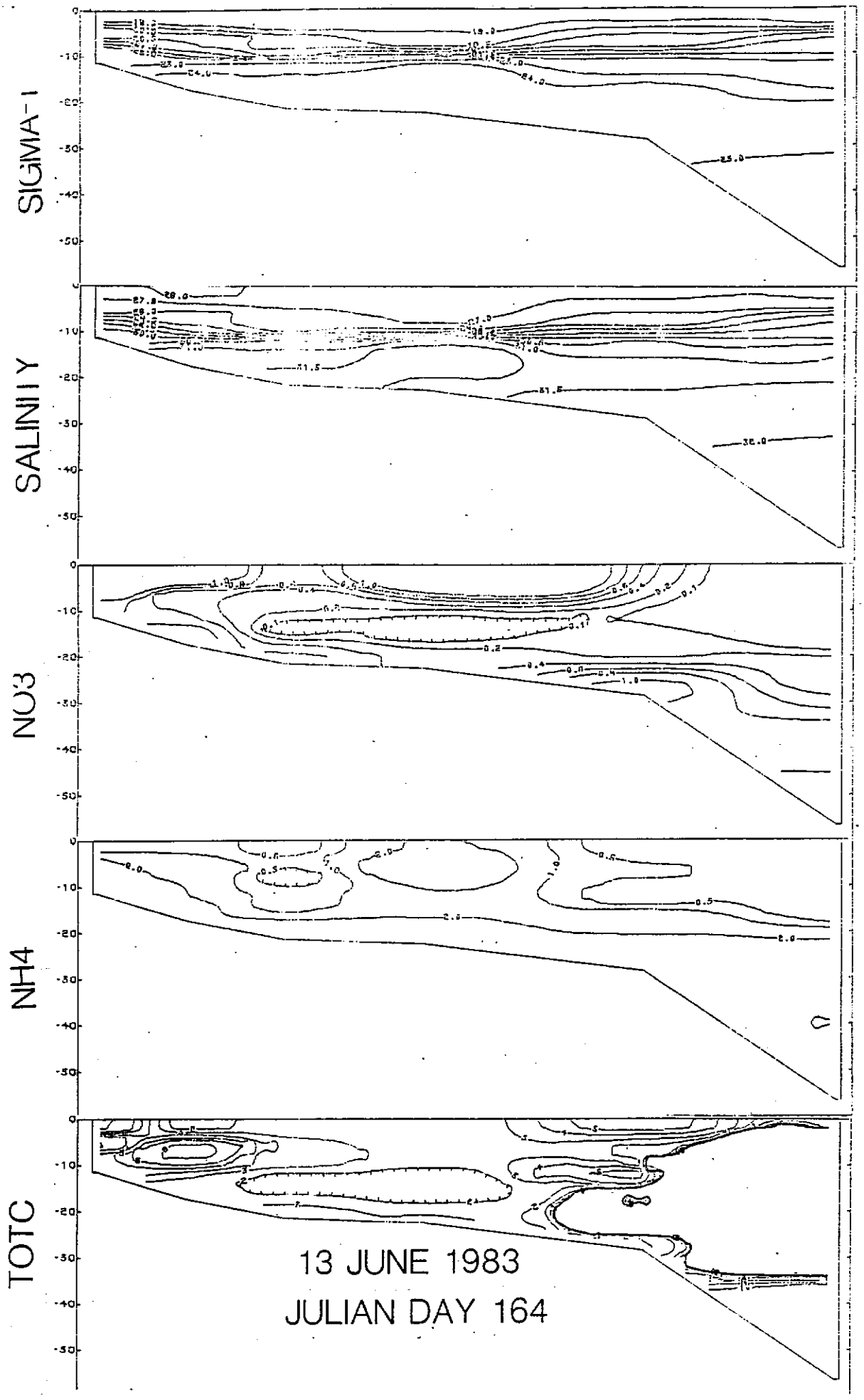

FIGURE 7

TRANSECT MONITORING

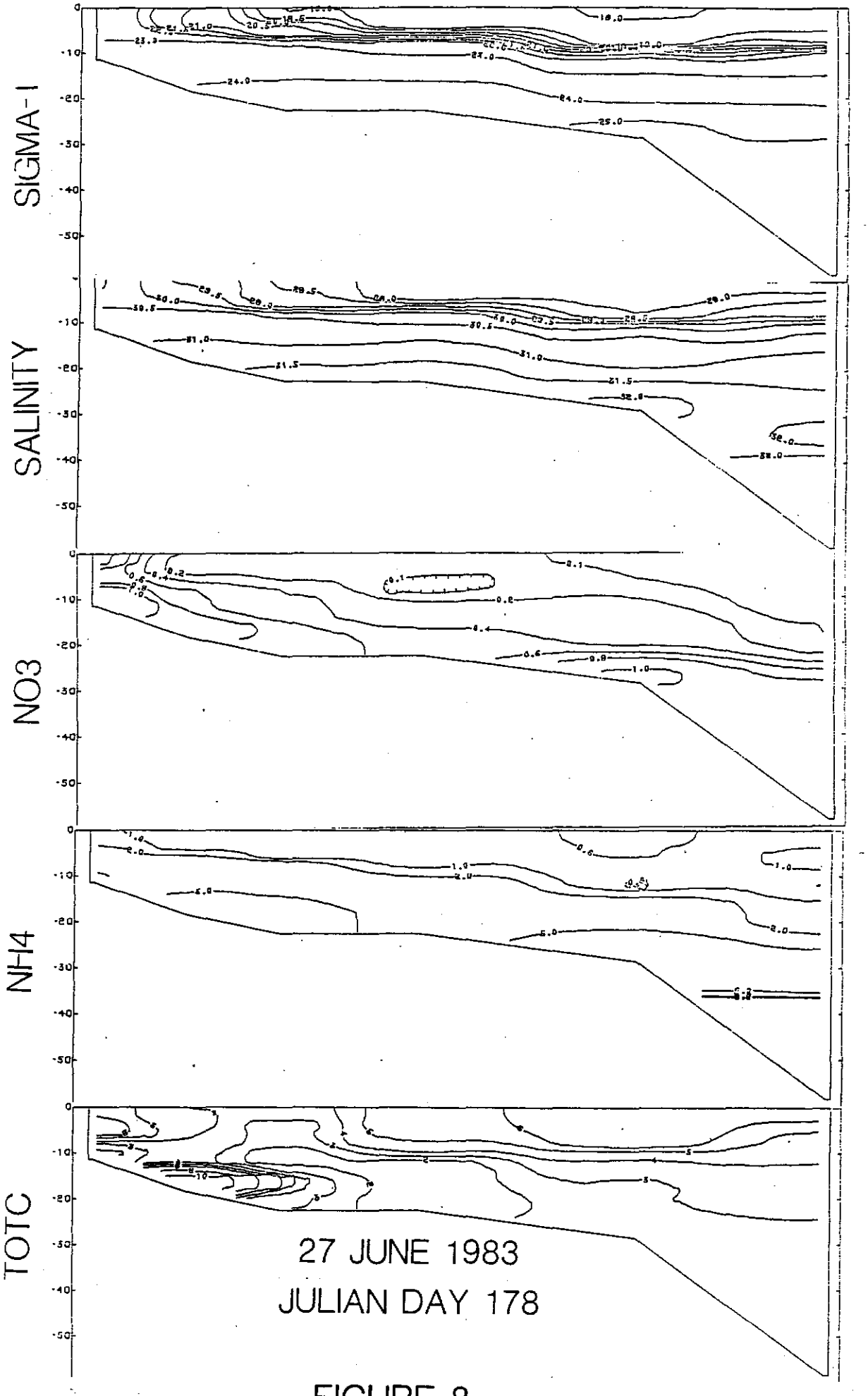

27 JUNE 1983

JULIAN DAY 178

FIGURE 8

TRANSECT MONITORING

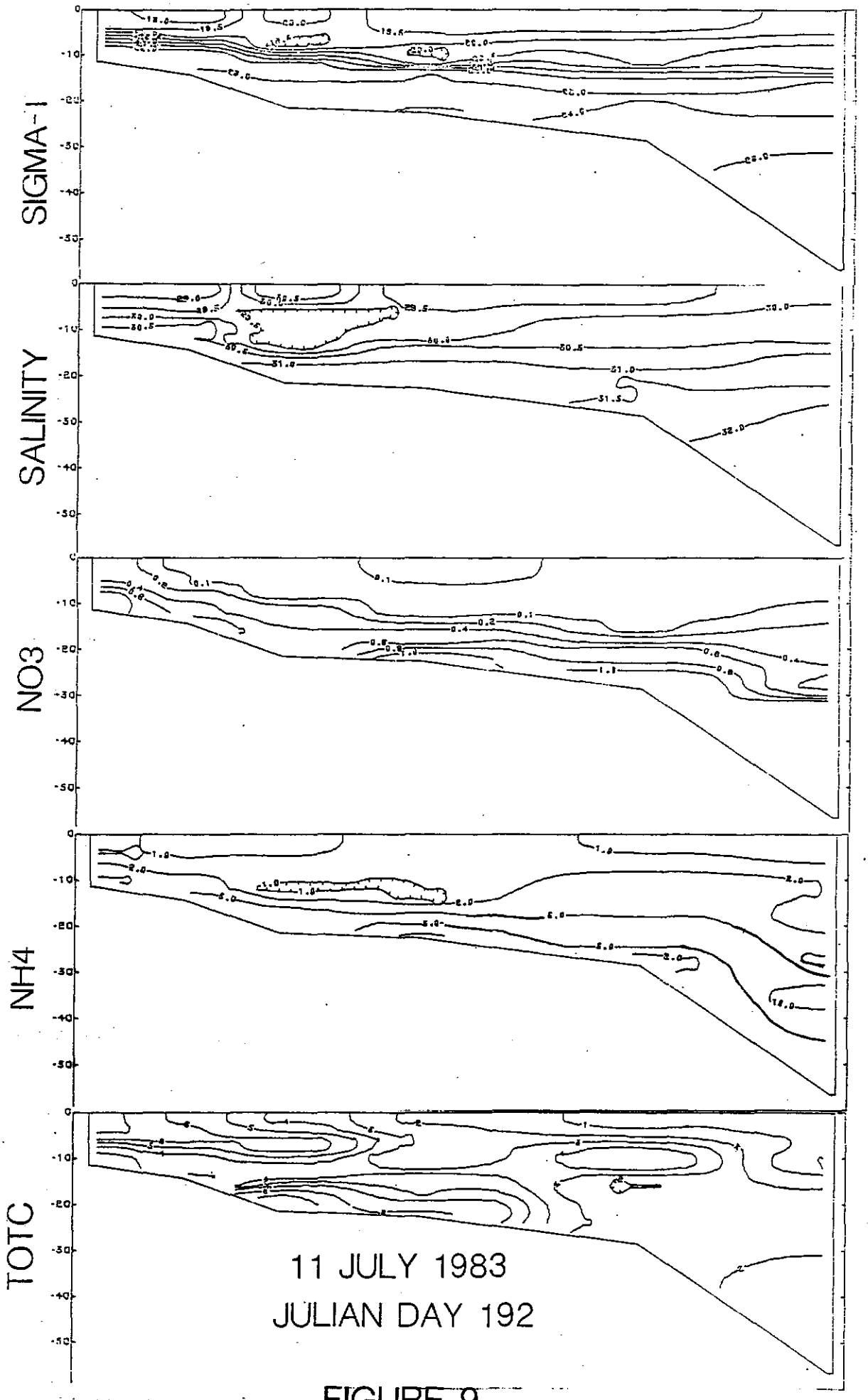

11 JULY 1983

JULIAN DAY 192

FIGURE 9

TRANSECT MONITORING

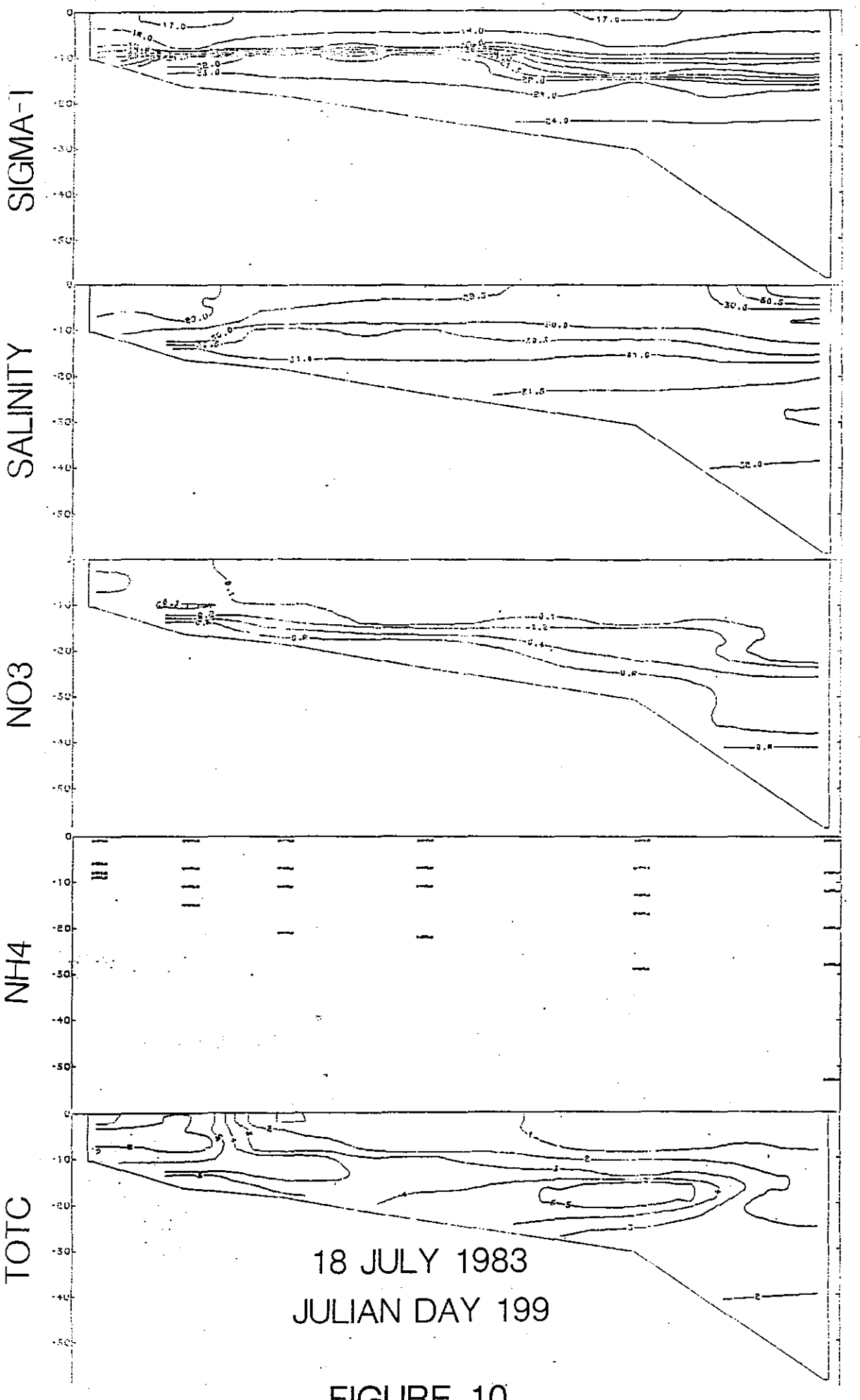

18 JULY 1983

JULIAN DAY 199

FIGURE 10

TRANSECT MONITORING

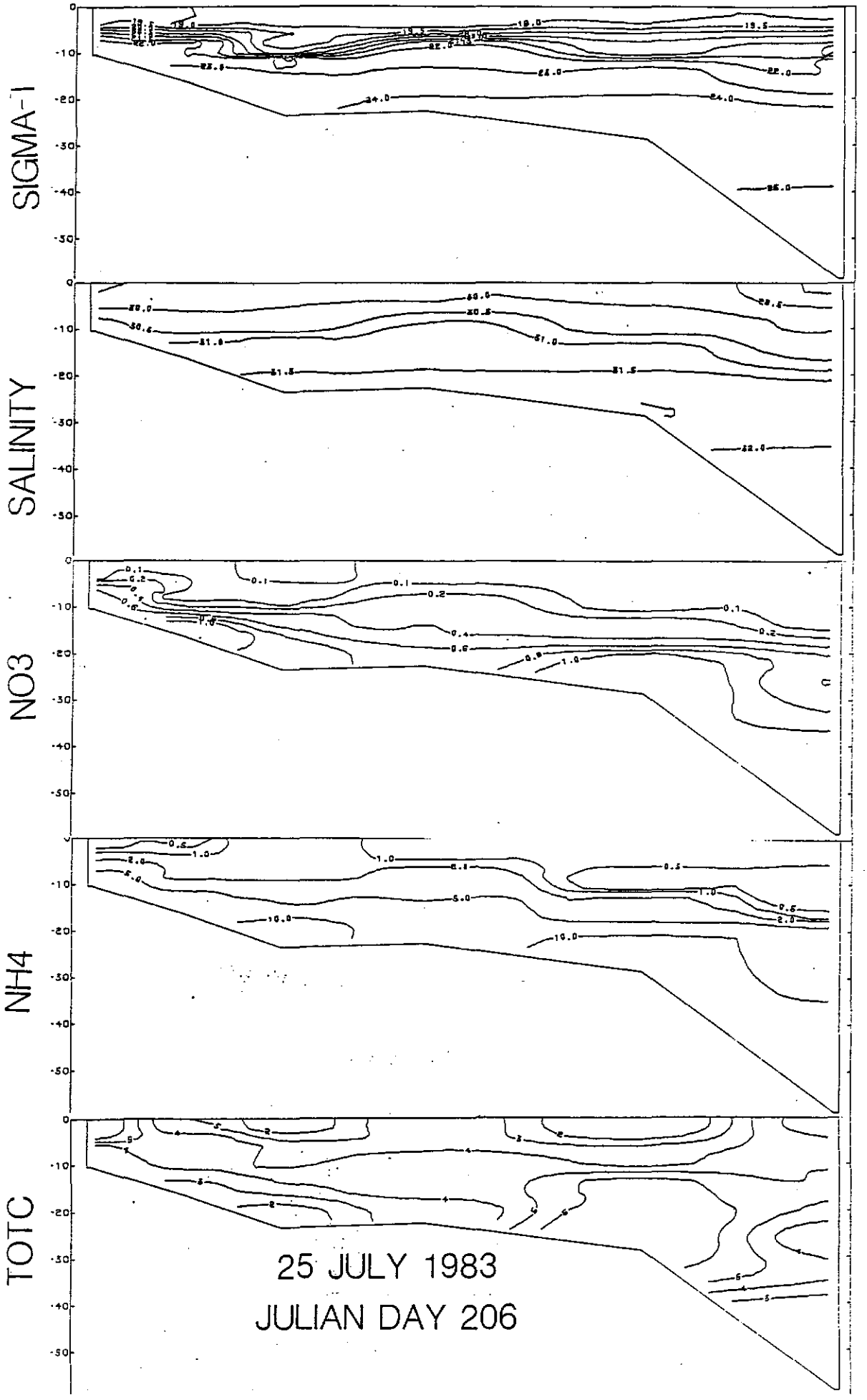

FIGURE 11

TRANSECT MONITORING

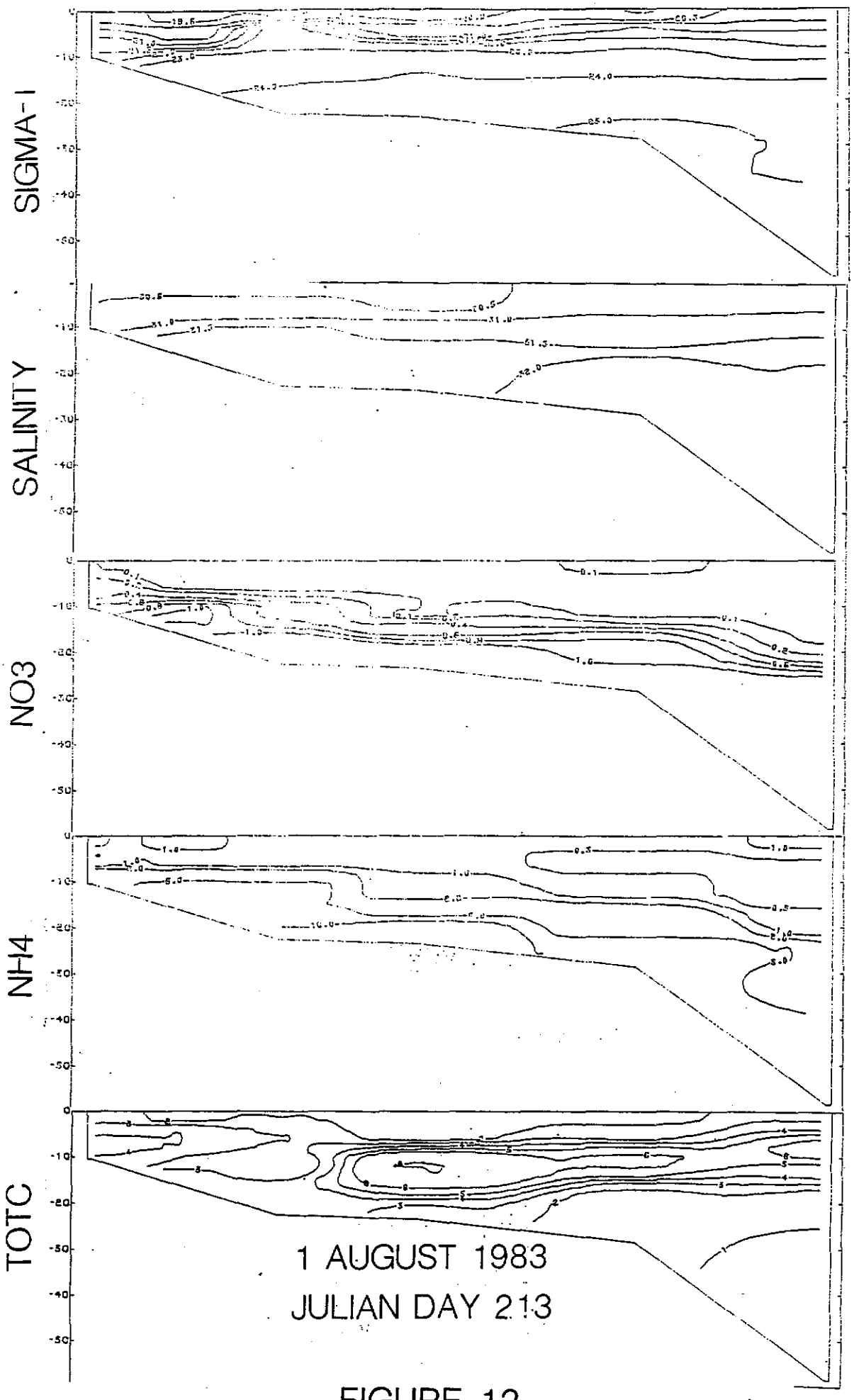

1 AUGUST 1983

JULIAN DAY 213

FIGURE 12

TRANSECT MONITORING

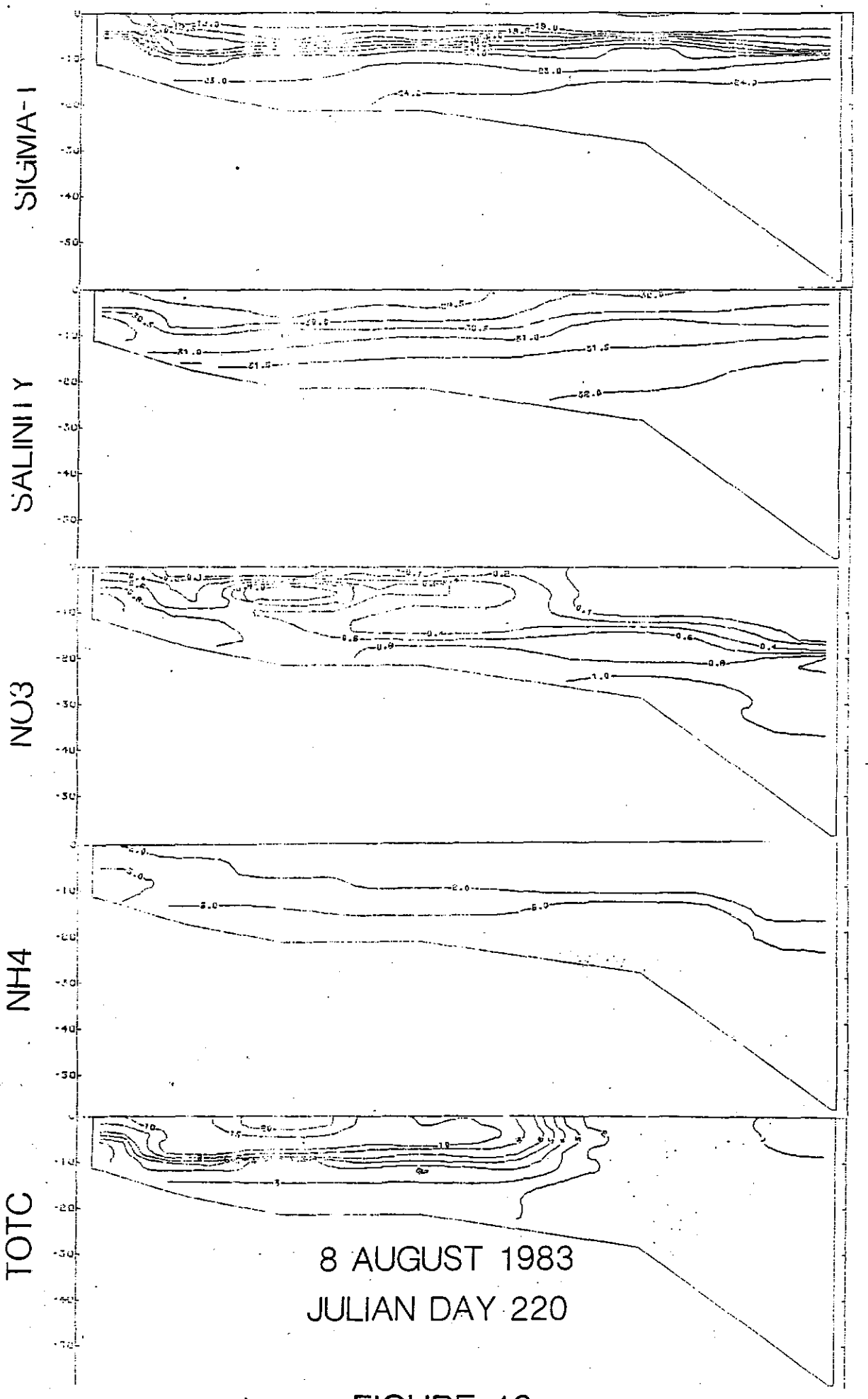

8 AUGUST 1983

JULIAN DAY 220

FIGURE 13

TRANSECT MONITORING

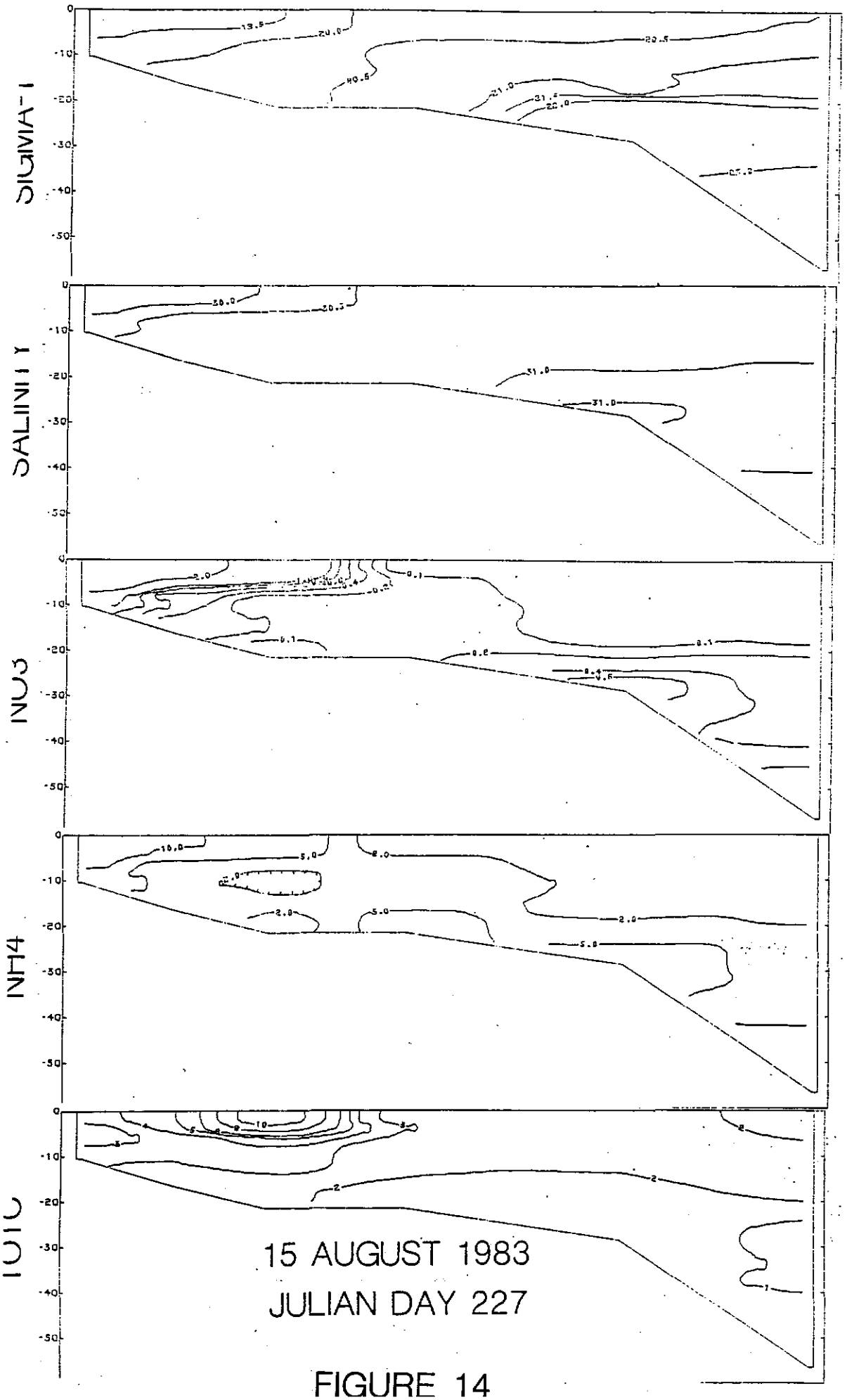

FIGURE 14

TRANSECT MONITORING

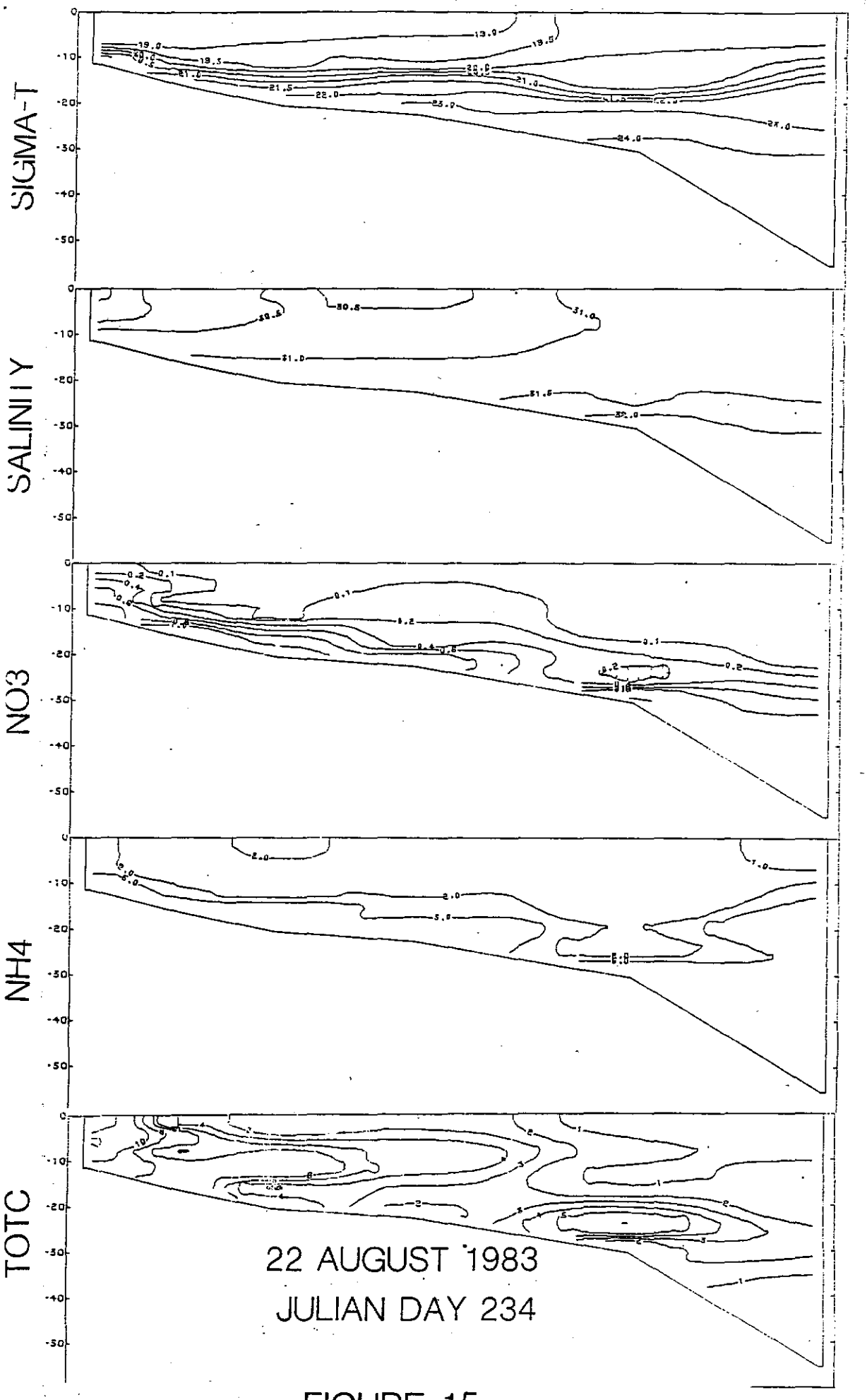

22 AUGUST 1983

JULIAN DAY 234

FIGURE 15

TRANSECT MONITORING

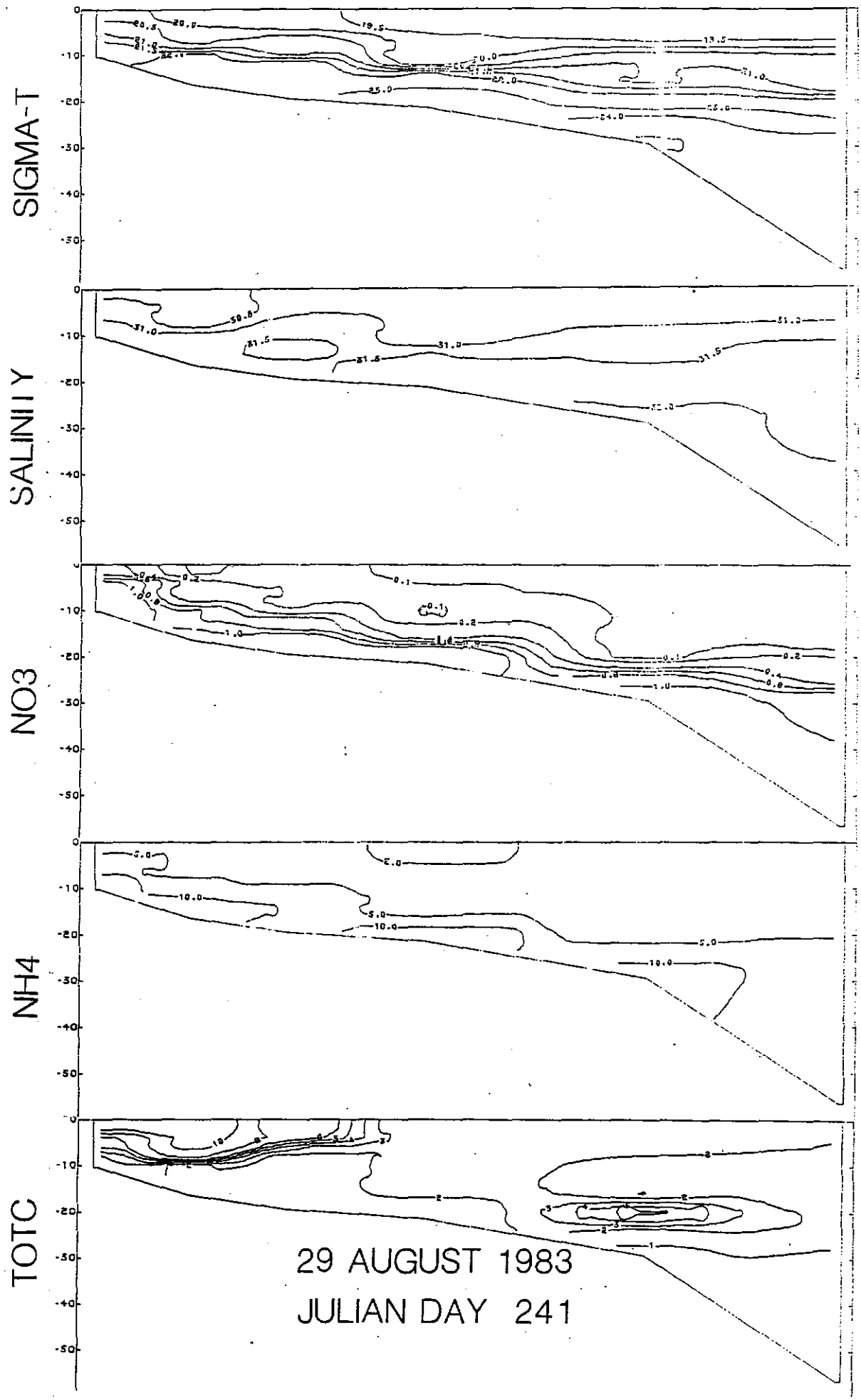

29 AUGUST 1983

JULIAN DAY 241

FIGURE 16

TRANSECT MONITORING

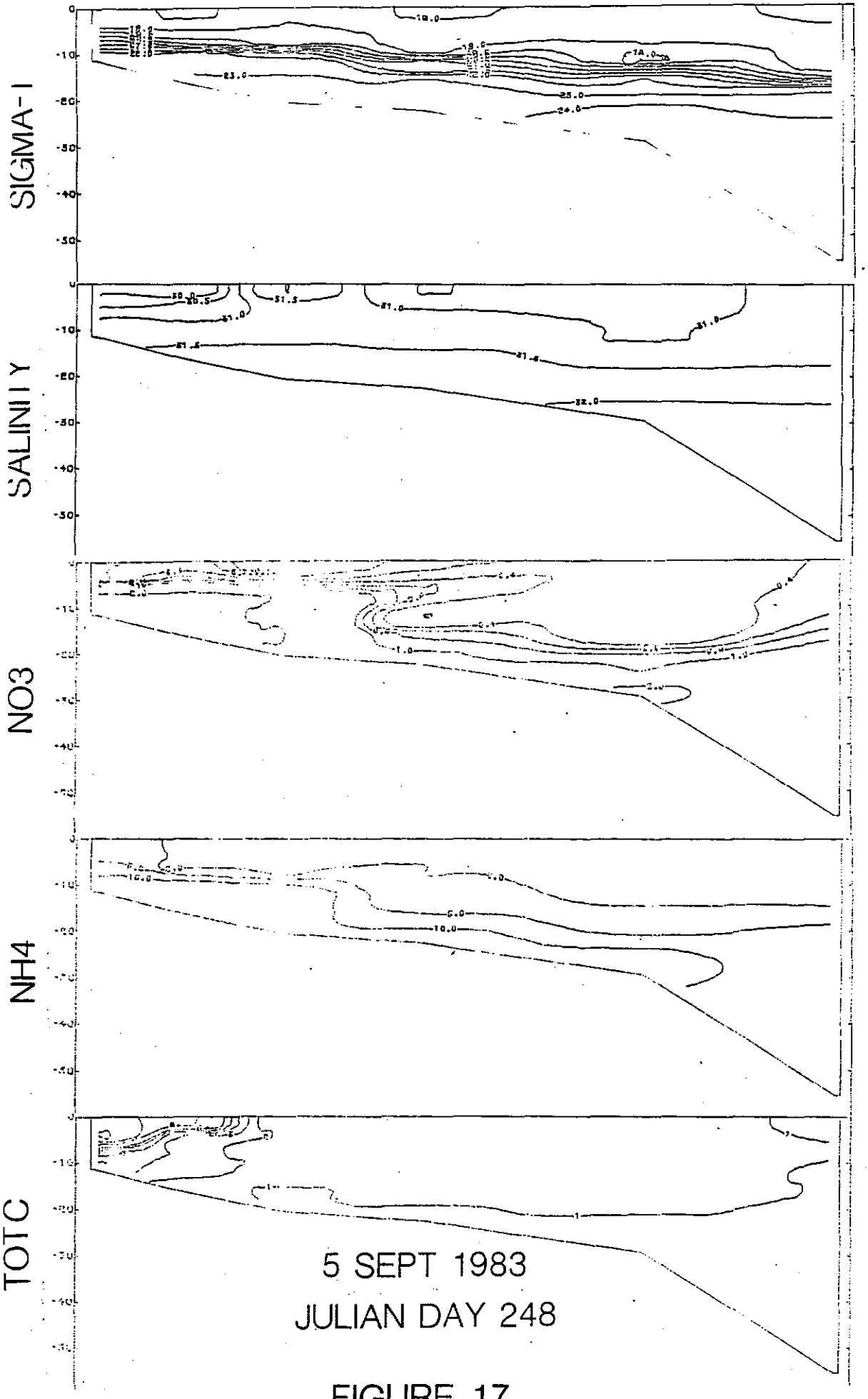

5 SEPT 1983

JULIAN DAY 248

FIGURE 17

TRANSECT MONITORING

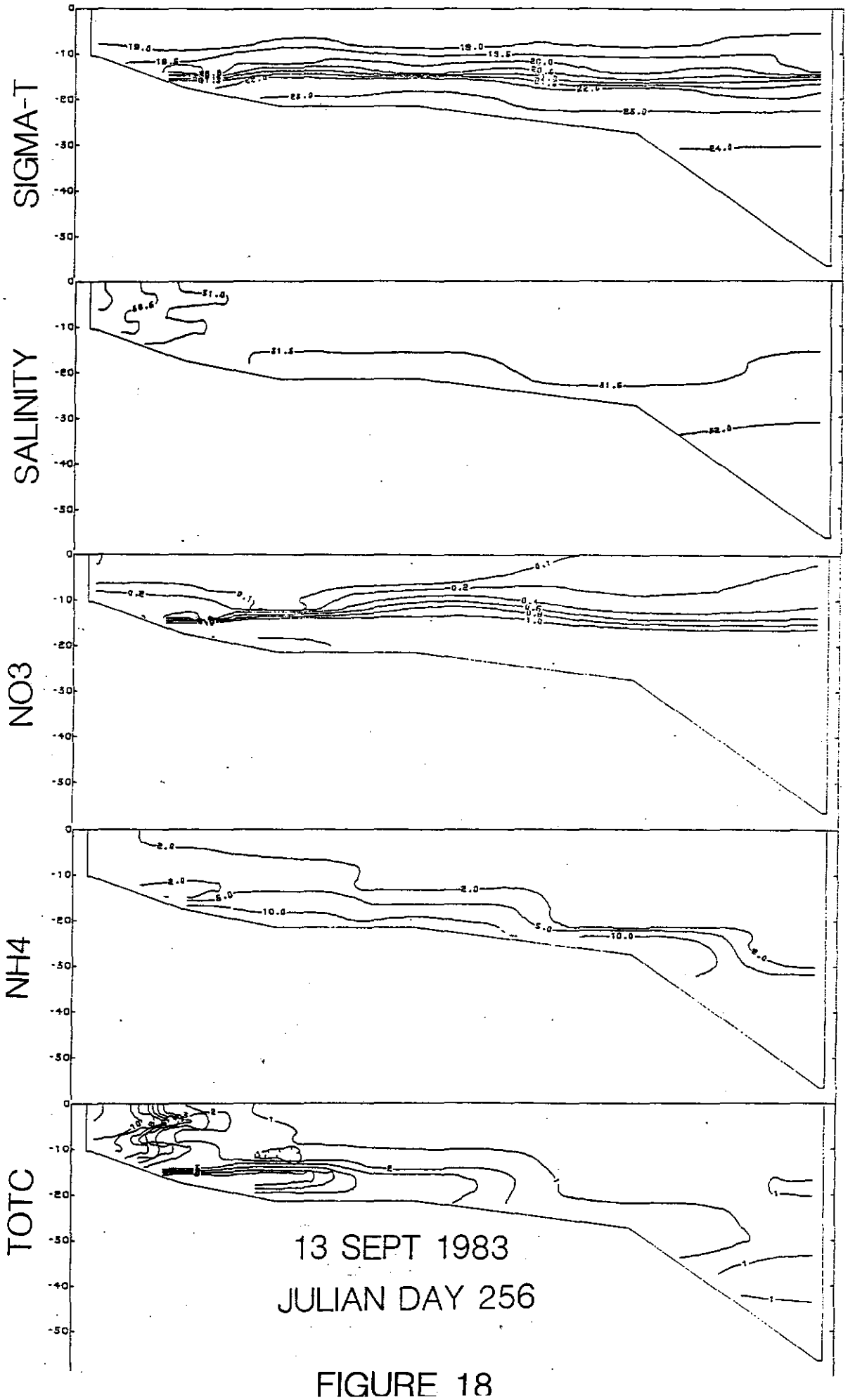

13 SEPT 1983

JULIAN DAY 256

FIGURE 18

TRANSECT MONITORING

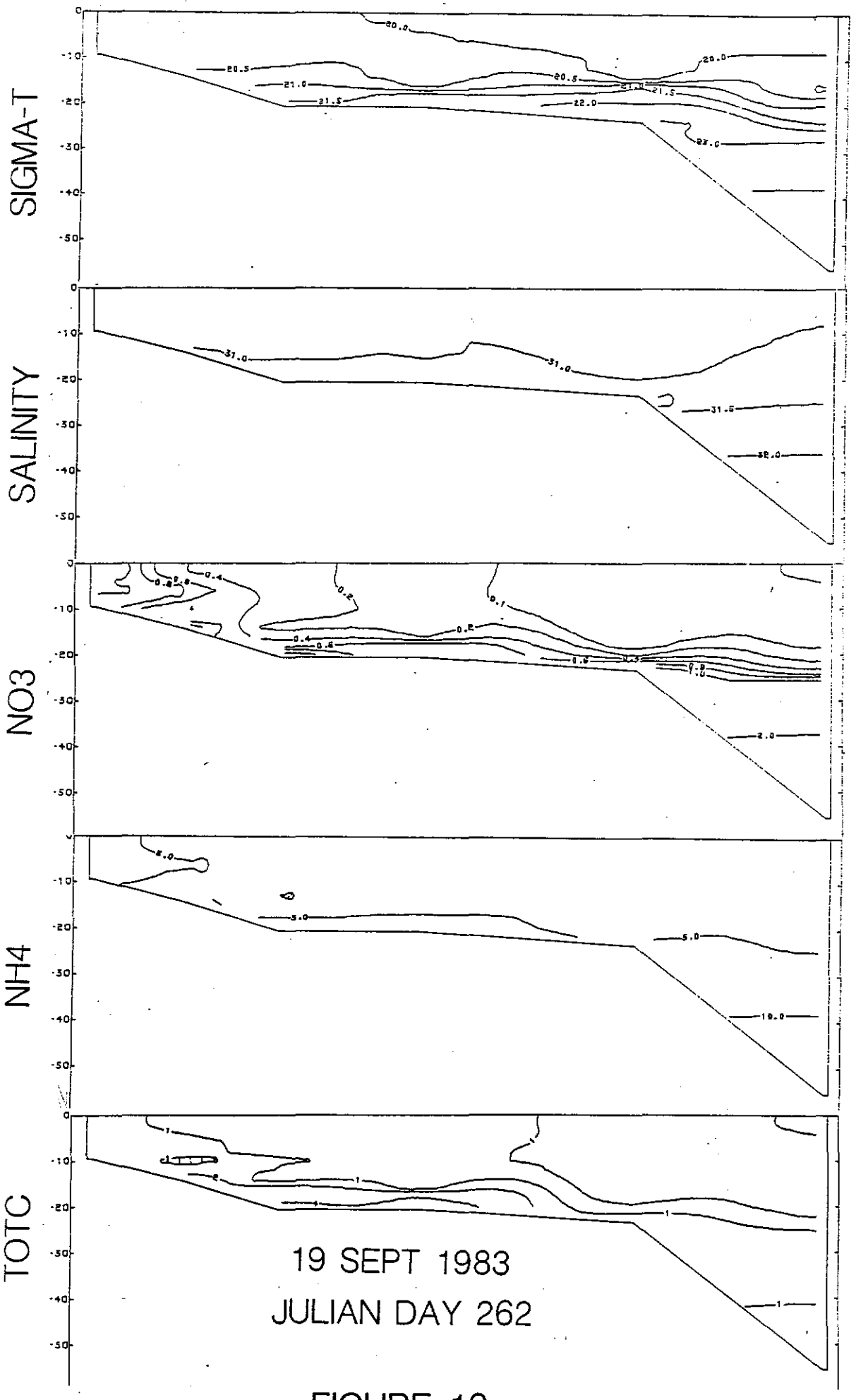

19 SEPT 1983

JULIAN DAY 262

FIGURE 19

LONG BRANCH PIER MONITORING

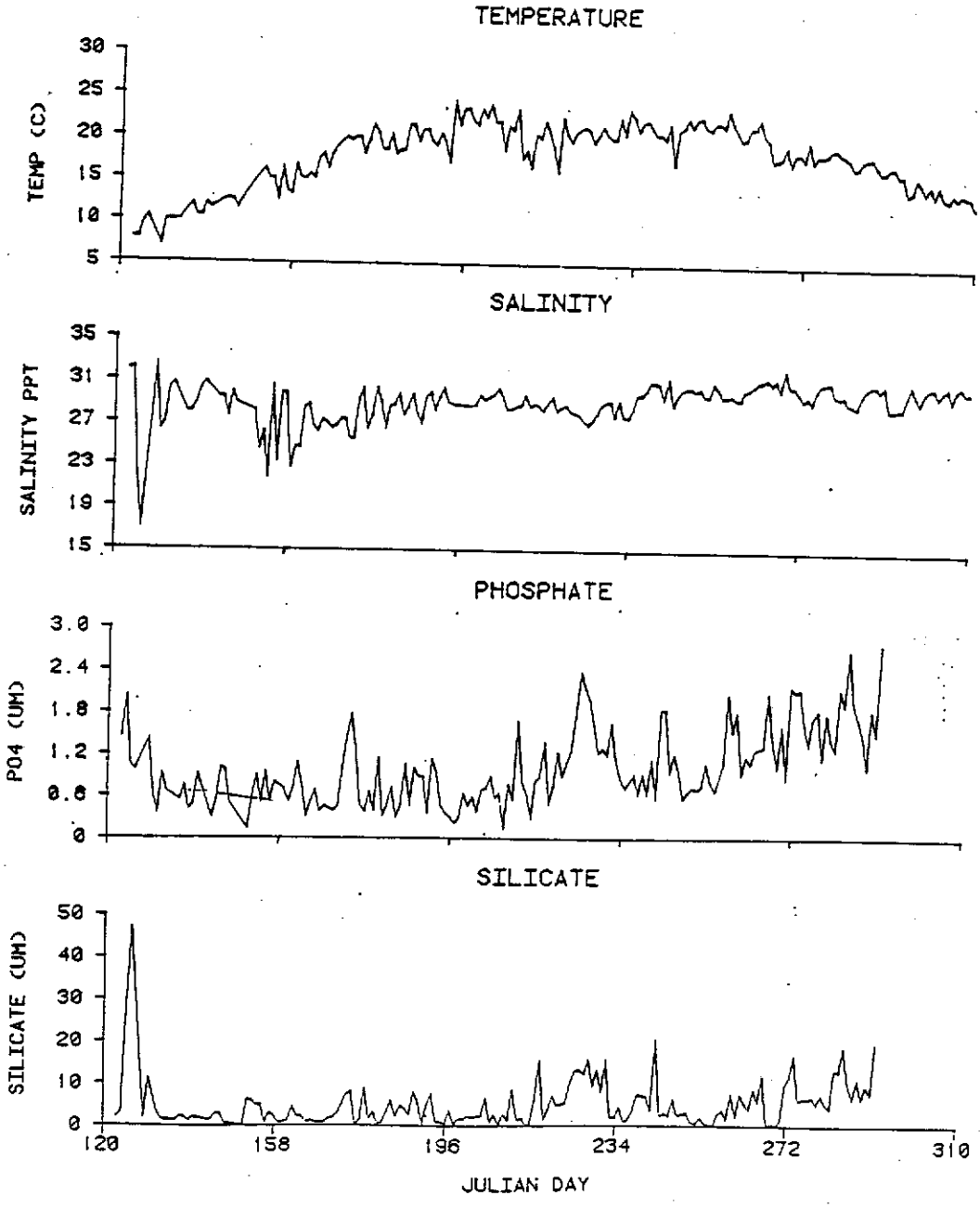

FIGURE 20

LONG BRANCH PIER MONITORING

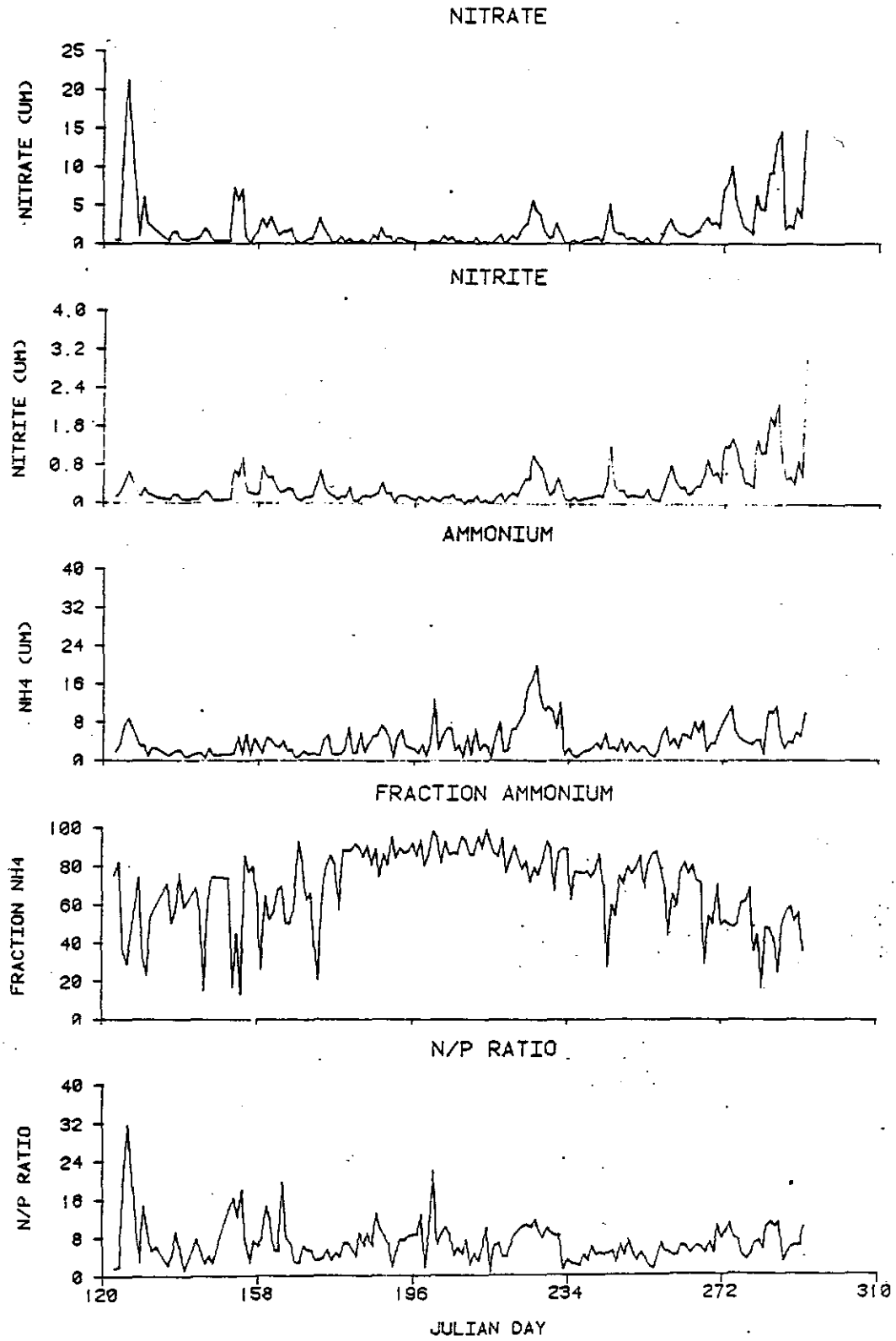

FIGURE 21

LONG BRANCH PIER MONITORING

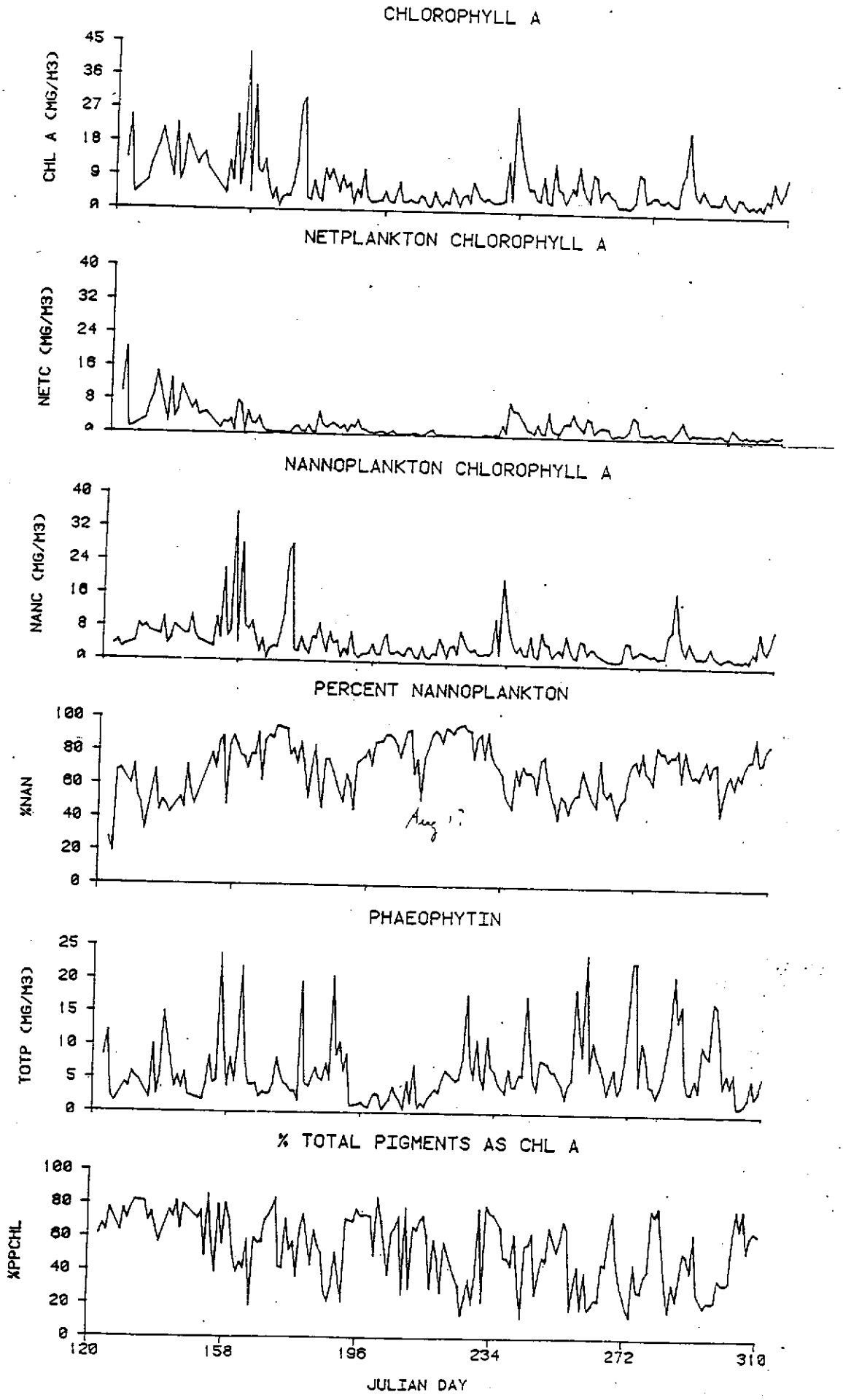

FIGURE 22